

# Constraints on a generalized deceleration parameter from cosmic chronometers and its thermodynamic implications

Abdulla Al Mamon<sup>1,\*</sup> and Subhajit Saha<sup>2,†</sup>

<sup>1</sup>*Manipal Centre for Natural Sciences, Manipal University, Manipal-576104, India*

<sup>2</sup>*Department of Physical Sciences, Indian Institute of Science Education and Research Kolkata, Mohanpur 741246, India*

In this paper, we have proposed a generalized parametrization for the deceleration parameter  $q$  in order to study the evolutionary history of the universe. We have shown that the proposed model can reproduce three well known  $q$ -parametrized models for some specific values of the model parameter  $\alpha$ . We have used the latest compilation of the Hubble parameter measurements obtained from the cosmic chronometer (CC) method (in combination with the local value of the Hubble constant  $H_0$ ) and the Type Ia supernova (SNIa) data to place constraints on the parameters of the model for different values of  $\alpha$ . We have found that the resulting constraints on the deceleration parameter and the dark energy equation of state support the  $\Lambda$ CDM model within  $1\sigma$  confidence level at the present epoch. Finally, we have given a thermodynamic motivation for such a parametrization by showing that our model is well consistent with the generalized second law of thermodynamics as well as thermodynamic equilibrium.

PACS numbers: 98.80.Hw, 98.80.-k, 98.80.Es

Keywords: deceleration parameter, parametrization, cosmic acceleration, cosmic chronometer, generalized second law, thermodynamic equilibrium

## I. INTRODUCTION

The late-time accelerated expansion phase of the universe is one of the biggest challenges in modern cosmology. A large number of cosmological observations [1–12] have strongly confirmed the current accelerated expansion phase of the universe. All of these observations also strongly suggest that the observed cosmic acceleration is rather a recent phenomenon and the universe was decelerating in the past. In the literature, the most accepted idea is that an exotic component of the matter sector with large negative pressure, dubbed as “dark energy”, is responsible for this acceleration. According to recent observational data, almost 68.3% of the total energy budget of the universe at the current epoch is filled with dark energy while 26.8% with dark matter and remaining 4.9% being the baryonic matter and radiation [13–15]. However, understanding the origin and nature of the dark sectors (dark energy and dark matter) is still a mystery. Different possibilities have been explored in order to find an explanation of the late-time observed cosmic acceleration and for some excellent reviews on dark energy models, one can refer to [16–20]. The simplest and consistent with most of the observations is the  $\Lambda$ CDM (cosmological constant  $\Lambda$  with pressureless cold dark matter) model where the constant vacuum energy density serves as the dark energy candidate. However, the models based upon cosmological constant suffer from two serious drawbacks, namely, the *fine tuning* and the cosmological *coincidence* problems [21, 22]. Therefore, most of the recent research is aimed towards finding a suitable cosmologically viable model of dark energy.

Parameterization of the deceleration parameter  $q$  is a useful tool towards a more complete characterization of the evolution history of the universe. Several well-known parameterizations for the deceleration parameter have been proposed so far (for a review, see [23–36]).

In the next section, we have proposed a generalized model for the deceleration parameter in order to explore late-stage evolution of the universe. One of the main properties of this model is that it can reproduce three popular  $q$ -parametrized models for some specific values of the model parameter. The constraints on the model parameters of our model have also been obtained using the SNIa, CC and  $H_0$  datasets. We have shown that the present model describes the evolution of the universe from an early decelerated phase ( $q > 0$ ) to an accelerated phase ( $q < 0$ ) at the present epoch for the combined dataset (SNIa+CC+ $H_0$ ).

---

\*Electronic address: [abdulla.mamon@manipal.edu](mailto:abdulla.mamon@manipal.edu)

†Electronic address: [subhajit1729@gmail.com](mailto:subhajit1729@gmail.com)

Given the strong interrelation between gravity and thermodynamics [37–40], a cosmological model which complies with the laws of thermodynamics, particularly, the (generalized) second law as well as thermodynamic equilibrium, in addition to fitting the observational data reasonably well, has a greater appeal as compared to other models which do not satisfy the same. In this paper, we have also undertaken such a thermodynamic study. In this regard, it is worthwhile to note that we shall only consider the entropies of the apparent horizon plus the fluid inside it and not the entropy of scalar fields as we assume these fields are in a pure quantum state and consequently their entropy vanishes altogether.

The organization of the paper is as follows. In section II, we have described the phenomenological model considered here. In section III, we have described the observational datasets (including their analysis methods) adopted in this work and discussed the results in section IV. Section V explores the thermodynamic implications of considering such a phenomenological parametrization for  $q$ . Finally, in section VI, we have summarized the conclusions of this work.

## II. THEORETICAL MODEL

We have assumed a homogeneous, isotropic and spatially flat Friedmann-Robertson-Walker (FRW) universe which is characterized by the following line element

$$ds^2 = dt^2 - a^2(t)[dr^2 + r^2(d\theta^2 + \sin^2\theta d\phi^2)] \quad (1)$$

where,  $a(t)$  is the scale factor of the universe which is scaled to be unity at the present epoch. In a spatially flat FRW geometry, the corresponding Einstein field equations take the form

$$3H^2 = 8\pi G(\rho_m + \rho_{de}) \quad (2)$$

$$2\dot{H} + 3H^2 = -8\pi G p_{de} \quad (3)$$

where  $H = \frac{\dot{a}}{a}$  is the Hubble parameter and the dot implies derivative with respect to the cosmic time  $t$ . Here,  $\rho_m$  represents the energy density of the dust matter while  $\rho_{de}$  and  $p_{de}$  represent the energy density and pressure of the dark energy respectively.

Also, the conservation equations for the dark energy and matter field are

$$\dot{\rho}_{de} + 3H(\rho_{de} + p_{de}) = 0 \quad (4)$$

$$\dot{\rho}_m + 3H\rho_m = 0 \quad (5)$$

In cosmology, the deceleration parameter  $q$  plays an important role in describing the nature of the expansion of the universe. Usually, it is parametrized as

$$q(z) = q_0 + q_1 F(z) \quad (6)$$

where  $q_0, q_1$  are constants and  $F(z)$  is a function of the redshift  $z$ . In fact, various functional forms of  $F(z)$  have been proposed in the literature [23–36] which can provide a satisfactory solution to some of the cosmological problems. Few popular  $q(z)$  models are: (i)  $q(z) = q_0 + q_1 z$ , (ii)  $q(z) = q_0 + q_1 \ln(1+z)$ , (iii)  $q(z) = q_0 + q_1 \left(\frac{z}{1+z}\right)$  and many more. However, some of these parametrizations diverge at  $z \rightarrow -1$  and others are valid for  $z < 1$  only. Recently, Mamon and Das [32, 33] proposed divergence-free parametrizations of  $q(z)$  to investigate the whole expansion history of the universe. They have shown that such models are more consistent with the recent observational data for some restrictions on model parameters. Therefore, search is still on for an appropriate functional form of  $q(z)$  that will describe the evolutionary history of the universe and fit well in dealing with cosmological challenges.

In order to close the system of equations as well as to extend the  $q$ -parametrizations above, in the present work, we propose

$$q(z) = q_0 - q_1 \left[ \frac{(1+z)^{-\alpha} - 1}{\alpha} \right] \quad (7)$$

where  $q_0$ ,  $q_1$  and  $\alpha$  are arbitrary model parameters. It deserves to mention here that  $q_0$  denotes the present value of  $q$ , and  $q_1$  denotes the derivative of  $q$  with respect to the redshift  $z$ . From equation (7), it is straightforward to show that the deceleration parameters given by examples (i)-(iii) are fully recovered in the following limits:

$$q(z) = \begin{cases} q_0 + q_1 z, & \text{for } \alpha = -1 \\ q_0 + q_1 \ln(1+z), & \text{for } \alpha \rightarrow 0 \\ q_0 + q_1 \left(\frac{z}{1+z}\right), & \text{for } \alpha = +1 \end{cases} \quad (8)$$

Thus, the new parametrization of  $q(z)$  covers a wide range of popular theoretical models (for  $\alpha = \pm 1$  and  $\alpha \rightarrow 0$ ) and also provides a new range of cosmological solutions in a more general framework for  $\alpha \neq -1, 0, +1$ . It is important to note that for the limit  $\alpha \rightarrow 0$ , we have used the equality,  $\lim_{\epsilon \rightarrow 0} \left[ \frac{x^\epsilon - 1}{\epsilon} \right] = \ln x$ . It deserves mention here that our parametrization is not valid at  $z = 0$ .

The deceleration parameter and the Hubble parameter are related by the following equation

$$H(z) = H_0 \exp \left( \int_0^z \frac{1 + q(x)}{1 + x} dx \right) \quad (9)$$

where  $H_0$  indicates the present value of the Hubble parameter. Using equations (7) and (9), the Friedmann equation for our generalized model can be obtained as

$$H(z) = H_0 (1+z)^{(1+q_0+\frac{q_1}{\alpha})} \exp \left[ \frac{q_1}{\alpha^2} \{ (1+z)^{-\alpha} - 1 \} \right] \quad (10)$$

It should be noted that the present mechanism can also be treated as parameterization of the Hubble parameter which can be constrained from observational Hubble data directly.

For this model, we obtained the expression for the equation of state parameter as

$$w_{de} = \frac{p_{de}}{\rho_{de}} = \frac{2q(z) - 1}{3 - 3\Omega_{m0}(1+z)^{1-2q_0-\frac{2q_1}{\alpha}} \exp \left[ \frac{2q_1}{\alpha^2} \{ 1 - (1+z)^{-\alpha} \} \right]} \quad (11)$$

where  $\Omega_{m0}$  indicates the present value of the density parameter of the matter component.

The behavior and the main cosmological characteristics of the model given in equation (7) strongly depend on the model parameters ( $q_0$ ,  $q_1$  and  $\alpha$ ). In the next section, using different observational datasets, we have constrained the model parameters ( $q_0$ ,  $q_1$ ) for some specific values of  $\alpha$ . In this work, we have worked with values ( $\alpha \neq -1, 0, +1$ ) as these particular  $q(z)$  models given in equation (8) has been studied extensively.

### III. DATA ANALYSIS METHODS

In this section, we have briefly discussed the datasets considered in our analysis, namely Type Ia Supernova (SNIa) and new dataset of Hubble parameter obtained with the cosmic chronometer (CC) method, in combination with the local value of  $H_0$ . In the following, we have described how these datasets are included into the  $\chi^2$  analysis.

#### A. Cosmic chronometer dataset and local value of the Hubble parameter

The *cosmic chronometers* (CC) approach was first introduced by [41] to measure  $H(z)$ . It uses the relative ages of the most massive and passively evolving galaxies to measure  $\frac{dz}{dt}$ , from which  $H(z)$  is deduced. In this work, we have used the latest updated list of Hubble parameter dataset [42–46] obtained through the CC approach, comprising 30 measurements spanning the redshift range  $0 < z < 2$ , recently compiled in [42, 43]. In our analysis, we have also included the recently measured local value of Hubble parameter given by Planck analysis ( $H_0 = 67.3 \pm 1.2$  km/s/Mpc) [13]. We have obtained the constraints on the model parameters by minimizing the following  $\chi^2$  function

$$\chi_H^2 = \sum_{i=1}^{30} \frac{[H^{obs}(z_i) - H^{th}(z_i, H_0, \theta)]^2}{\sigma_H^2(z_i)}, \quad (12)$$

where  $H^{obs}$  and  $H^{th}$  are the observed and theoretical values of the Hubble parameter respectively. Also,  $\sigma_H$  represents the uncertainty associated with each measurement of  $H$  and  $\theta$  denotes the model parameter.

### B. Type Ia Supernova dataset

Data from the Type Ia Supernova was the first indication for cosmic acceleration and it is very useful to test the cosmological models. So, along with the CC dataset, we have also utilized the 31 binned distance modulus data sample of the recent “joint light curve” (JLA) analysis in the present work [47]. For this dataset, the  $\chi^2$  is defined as (see [48] for more details)

$$\chi_{SNIa}^2 = A(\theta) - \frac{B^2(\theta)}{C} - \frac{2\ln 10}{5C} B(\theta) - Q \quad (13)$$

with

$$A(\theta) = \sum_{\alpha, \beta} (\mu^{th} - \mu^{obs})_{\alpha} (Cov)_{\alpha\beta}^{-1} (\mu^{th} - \mu^{obs})_{\beta}, \quad (14)$$

$$B(\theta) = \sum_{\alpha} (\mu^{th} - \mu^{obs})_{\alpha} \sum_{\beta} (Cov)_{\alpha\beta}^{-1}, \quad (15)$$

$$C = \sum_{\alpha, \beta} (Cov)_{\alpha\beta}^{-1} \quad (16)$$

Here, “Cov” is the  $31 \times 31$  covariance matrix of the binned data sample,  $Q$  is a constant that does not depend on the model parameter  $\theta$  and hence has been ignored. Here,  $\mu^{obs}$  denotes the observed distance modulus, while  $\mu^{th}$  is for the theoretical one, which is defined as

$$\mu^{th} = 5 \log_{10} \left[ \frac{d_L(z)}{1 \text{Mpc}} \right] + 25 \quad (17)$$

where,

$$d_L(z) = \frac{(1+z)}{H_0} \int_0^z \frac{dx}{h(x)} \quad \text{and} \quad h = \frac{H}{H_0}. \quad (18)$$

Since the SNIa and CC are effectively independent observations, we can combine these datasets by adding together the  $\chi^2$  functions. Thus, the combined  $\chi^2$  can be expressed as

$$\chi^2 = \chi_{SNIa}^2 + \chi_H^2. \quad (19)$$

For the combined dataset (SNIa+CC+ $H_0$ ), we estimate the best-fit values of the model parameters by minimizing  $\chi^2$ . Then, we use the maximum likelihood method and take the combined likelihood function as  $\mathcal{L} = e^{-\frac{\chi^2}{2}}$ . The best-fit parameter values  $\theta^*$  are those that minimize the likelihood function

$$\mathcal{L}(\theta^*) = \exp \left[ -\frac{\chi^2(\theta^*)}{2} \right] \quad (20)$$

We can now plot the contours for different confidence levels, e.g.,  $1\sigma$  and  $2\sigma$ .

## IV. RESULTS OF THE DATA ANALYSIS

Figure 1 shows the  $1\sigma$  and  $2\sigma$  contours in  $q_0 - q_1$  plane for the generalized  $q$ -parametrization given by equation (7). We have found that the best-fit values of the free parameters ( $q_0$  and  $q_1$ ) for the CC+ $H_0$ , SNIa and SNIa+CC+ $H_0$  datasets are well fitted in the  $1\sigma$  confidence contour. We have also found that the constraints obtained on the parameter values by the joint analysis (SNIa+CC+ $H_0$ ) are very tight as compared to the constraints obtain from the CC+ $H_0$  dataset and the SNIa dataset independently. On the other hand, figure 2 and 3 show the plots of the marginalized likelihood as functions of the model parameters  $q_0$  and  $q_1$  respectively. It is observed from the likelihood plots that the likelihood functions are well fitted to a Gaussian distribution function for each dataset. The corresponding constraints

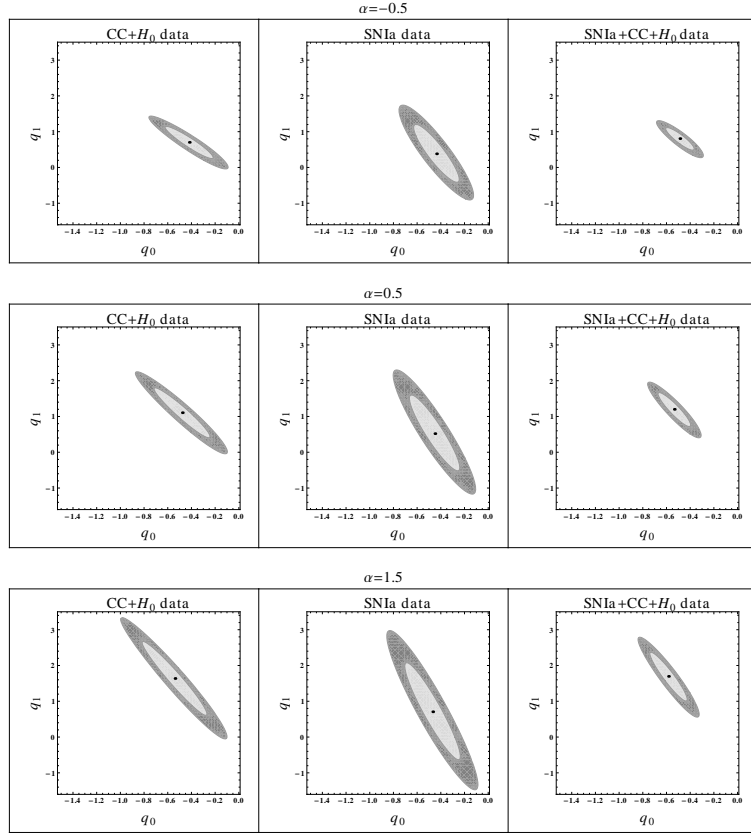


FIG. 1: This figure shows the  $1\sigma$  and  $2\sigma$  confidence contours for different choices of  $\alpha$  and using the various datasets (CC+ $H_0$ , SNIa and SNIa+CC+ $H_0$ ), as indicated in each panel. The upper, middle and lower panels are for  $\alpha = -0.5, 0.5$  and  $1.5$  respectively. In each panel, the large dot represents the best-fit values of the pair  $(q_0, q_1)$ .

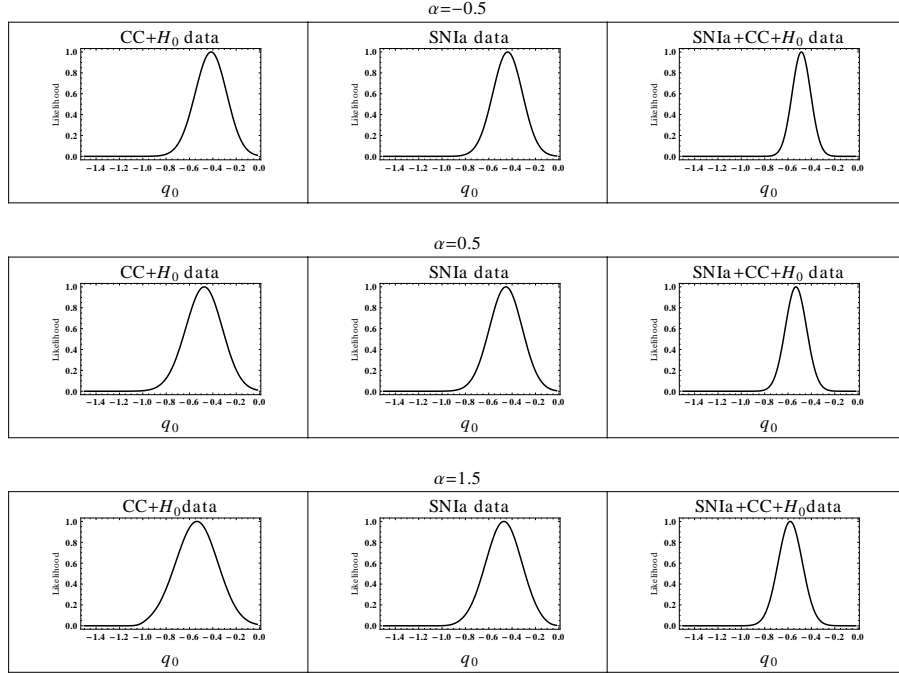


FIG. 2: This figure shows the marginalized likelihood function vs.  $q_0$  for different choices of  $\alpha$  using the various datasets, as indicated in each panel. The upper, middle and lower panels are for  $\alpha = -0.5, 0.5$  and  $1.5$  respectively.

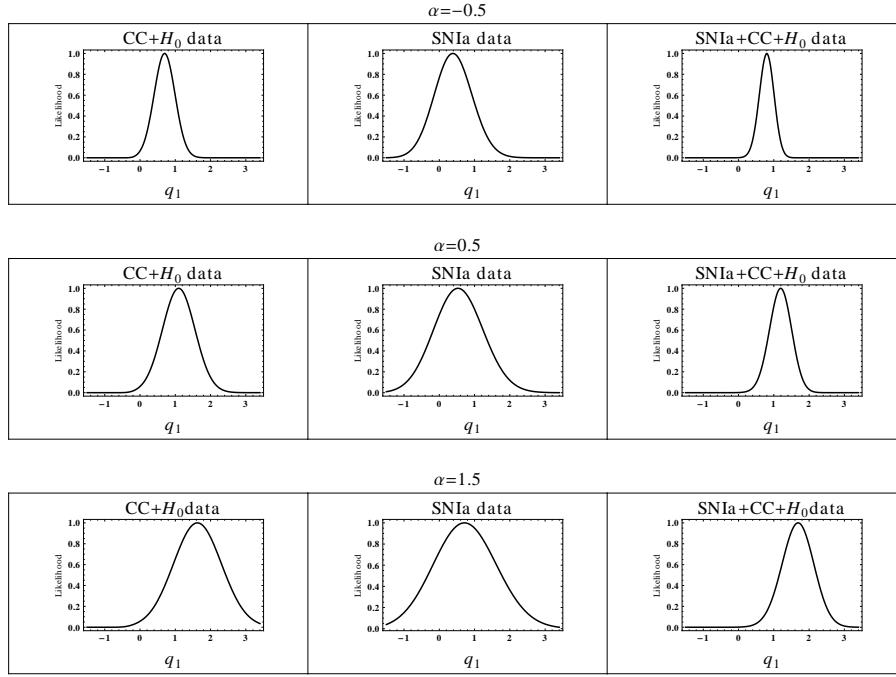


FIG. 3: This figure shows the marginalized likelihood function vs.  $q_1$  for different choices of  $\alpha$  using the various datasets, as indicated in each panel. The upper, middle and lower panels are for  $\alpha = -0.5, 0.5$  and  $1.5$  respectively.

TABLE I: Best fit values of the model parameters ( $q_0$  and  $q_1$ ) by considering different values of  $\alpha$ . For this analysis, we have considered CC+ $H_0$  dataset. Here,  $\chi_m^2$  is the minimum value of  $\chi^2$ .

$\alpha$	$q_0$	$q_1$	Constraints on $q_0$ and $q_1$ (within $1\sigma$ C.L.)	$\chi_m^2$
-0.5	-0.41	0.70	$-0.60 \leq q_0 \leq -0.21, 0.24 \leq q_1 \leq 1.08$	14.93
0.5	-0.48	1.10	$-0.70 \leq q_0 \leq -0.24, 0.39 \leq q_1 \leq 1.74$	14.72
1.5	-0.54	1.63	$-0.80 \leq q_0 \leq -0.27, 0.56 \leq q_1 \leq 2.61$	14.64

on model parameters are summarized in table I, II and III.

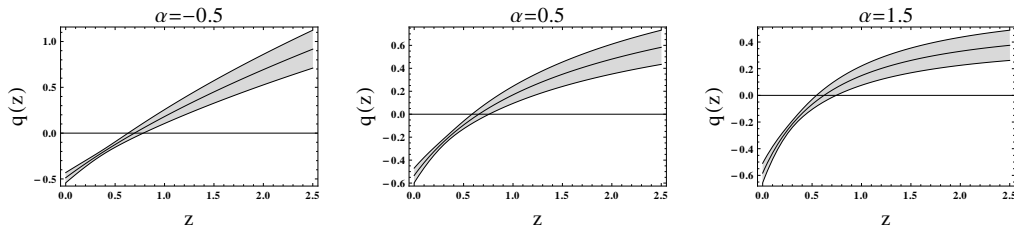
The evolution of the deceleration parameter  $q(z)$  with  $1\sigma$  error is shown in figure 4 by considering different values of  $\alpha$ . The reconstruction of  $q(z)$  is done by the combined (SNIa+CC+ $H_0$ ) dataset. It has been found that for the present model,  $q(z)$  shows a signature flip at the transition redshift  $z_t = 0.69_{-0.06}^{+0.09}$ ,  $0.65_{-0.07}^{+0.10}$ , and  $0.61_{-0.08}^{+0.12}$  within  $1\sigma$  errors for  $\alpha = -0.5, 0.5$  and  $1.5$  respectively. This is well consistent with the previous results given in [28, 32, 49–51], which is also in good agreement with the  $\Lambda$ CDM value ( $z_t \approx 0.7$ ). Similarly, the evolution of  $w_{de}(z)$  with  $1\sigma$  error is shown in figure 5 for the (SNIa+CC+ $H_0$ ) dataset, by considering different values of  $\alpha$ . It is observed from figure 5 that the present value of  $w_{de}(z)$  with  $1\sigma$  error is very close to  $-1$  in all cases (i.e.,  $w_{de}(z=0) = -0.94_{-0.05}^{+0.05}$ ,  $-0.99_{-0.06}^{+0.06}$  and  $-1.02_{-0.07}^{+0.07}$  for  $\alpha = -0.5, 0.5$  and  $1.5$  respectively). Therefore, the results are consistent with the  $\Lambda$ CDM model.

TABLE II: Best fit values of the model parameters for the analysis of SNIa dataset by considering different values of  $\alpha$ .

$\alpha$	$q_0$	$q_1$	Constraints on $q_0$ and $q_1$ (within $1\sigma$ C.L.)	$\chi_m^2$
-0.5	-0.43	0.38	$-0.61 \leq q_0 \leq -0.24, -0.47 \leq q_1 \leq 1.13$	32.82
0.5	-0.45	0.52	$-0.65 \leq q_1 \leq -0.25, -0.50 \leq q_1 \leq 1.55$	32.76
1.5	-0.47	0.70	$-0.68 \leq q_0 \leq -0.23, -0.67 \leq q_1 \leq 2.02$	32.70

TABLE III: Best fit values of the model parameters by considering different values of  $\alpha$ . This is for the SNIa+CC+ $H_0$  dataset.

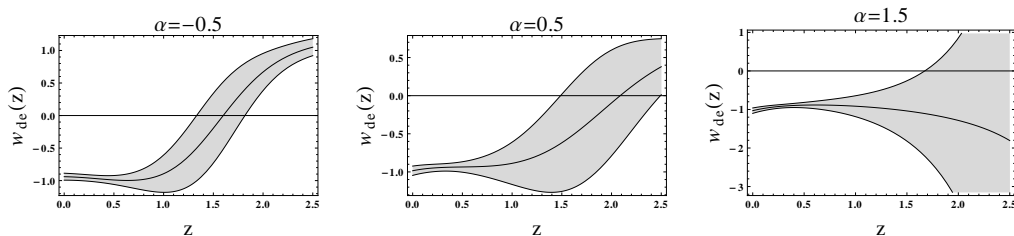
$\alpha$	$q_0$	$q_1$	Constraints on $q_0$ and $q_1$ (within $1\sigma$ C.L.)	$\chi_m^2$
-0.5	-0.48	0.81	$-0.60 \leq q_0 \leq -0.37, 0.49 \leq q_1 \leq 1.08$	49.26
0.5	-0.53	1.20	$-0.66 \leq q_0 \leq -0.40, 0.73 \leq q_1 \leq 1.64$	49.29
1.5	-0.58	1.69	$-0.71 \leq q_0 \leq -0.43, 1.01 \leq q_1 \leq 2.26$	49.55

FIG. 4: The evolution of deceleration parameter  $q(z)$  is shown for the SNIa+CC+ $H_0$  dataset by considering different values of  $\alpha$ , as indicated in each panel. In each panel, the central thin line and the light gray region represent the best fit curve and the  $1\sigma$  confidence level respectively.

## V. THERMODYNAMIC IMPLICATIONS

We shall now study the thermodynamic implications of considering a generalized form of the deceleration parameter as given in equation (7). In this regard, it will be sufficient to know whether the *generalized second law* (GSL) of thermodynamics and *thermodynamic equilibrium* (TE) hold good or not. While GSL should be satisfied throughout the evolution of any physical system (in our case the universe), TE should hold atleast during the late stages of the evolution [52]. Keeping these points in mind, let us consider our universe bounded by the cosmological (or dynamical) apparent horizon to be a macroscopic isolated physical system for which we shall attempt to verify the validity of GSL and TE.

Now, if  $S$  be the entropy of our system (horizon+cosmic fluid inside), then  $\text{GSL}^1$  and TE refer to the inequalities  $\dot{S} \geq 0$  and  $\ddot{S} < 0$  respectively. As stated above, the former should be true throughout the evolution of the universe, while the latter should hold at least during the final phases of its evolution. The total entropy  $S$  should be the sum of the entropy of the apparent horizon ( $S_A$ ) and that of the fluid inside the horizon ( $S_f$ ). Thus the two inequalities modify as  $\frac{d}{dt}(S_A + S_f) \geq 0$  and  $\frac{d^2}{dt^2}(S_A + S_f) < 0$ . At this point, it is worthwhile to mention that this type of thermodynamic study was first undertaken by Wang, Gong and Abdalla [54].

FIG. 5: The evolution of  $w_{de}(z)$  is shown for the SNIa+CC+ $H_0$  dataset by considering different values of  $\alpha$ , as indicated in each panel. In each panel, the central thin line and the light gray region represent the best fit curve and the  $1\sigma$  confidence level respectively. All the plots are for  $\Omega_{m0} = 0.3$ .

<sup>1</sup> The idea of incorporating the GSL in cosmology was first developed by Ram Brustein [53]. This second law is based on the conjecture that causal boundaries and not only event horizons have geometric entropies proportional to their area.

It is well known that the horizon entropy scales as its area, i.e.,

$$S_A = \left( \frac{c^3}{G\hbar} \right) \pi R_A^2, \quad (21)$$

where  $R_A = \frac{1}{H}$  is the location of the cosmological apparent horizon for a flat FRW universe. The temperature of the horizon is proportional to its surface gravity and is given by

$$T_A = \left( \frac{\hbar c}{\kappa_B} \right) \frac{1}{2\pi R_A}. \quad (22)$$

The temperature of the fluid ( $T_f$ ) is generally considered equal to the horizon temperature, i.e.,  $T_f = T_A$ , while the fluid entropy can be obtained from the Gibb's equation

$$T_f dS_f = dE_f + p dV_A, \quad (23)$$

where  $E_f = \rho V_A$  is the total entropy of the fluid inside the apparent horizon,  $V_A = \frac{4}{3}\pi R_A^3$  is the volume of the fluid, and  $\rho$  and  $p$  are, respectively, the energy density and the pressure of the cosmic fluid respectively.

Assuming without any loss of generality that  $8\pi$  and the constants  $c$ ,  $G$ ,  $\hbar$ , and  $\kappa_B$  are equal to unity, we have the expression for the first and the second time derivatives of the total entropy for a universe bounded by the apparent horizon as [54–56]

$$\begin{aligned} \dot{S} &= \frac{d}{dt}(S_A + S_f) \\ &= \frac{9\sqrt{3}}{16\sqrt{\rho}} \left( 1 + \frac{p}{\rho} \right)^2 \end{aligned} \quad (24)$$

and

$$\begin{aligned} \ddot{S} &= \frac{d^2}{dt^2}(S_A + S_f) \\ &= \frac{9}{16} \left( 1 + \frac{p}{\rho} \right) \left[ \left( 1 + \frac{p}{\rho} \right) \left( 1 + 6\frac{p}{\rho} \right) - \left( 5 + 3\frac{p}{\rho} \right) \frac{\dot{p}}{\dot{\rho}} \right] \end{aligned} \quad (25)$$

respectively.

It is evident from equation (24) that the GSL is valid throughout the evolution of the universe irrespective of the nature of the cosmic fluid chosen. As far as equation (25) is concerned, we need to write it in terms of the deceleration parameter  $q$  in order to be able to draw any interesting conclusion. It is remarkable to see that using the Friedmann and acceleration equations, and the definition

$$q = -\frac{\dot{H}}{H^2} - 1, \quad (26)$$

Eq. (25) can be expressed in terms of  $q$  and  $\frac{dq}{dz}$  as

$$\ddot{S} = \frac{1}{4} \left[ (1+q)(1+2q^2) - (2+q)(1+z)\frac{dq}{dz} \right]. \quad (27)$$

It should be noted that in deriving the above equation we have used the expression

$$\frac{\dot{p}}{\dot{\rho}} = \frac{1}{3(1+q)} \left[ (1+z)\frac{dq}{dz} + 2(1+q)^2 - 3(1+q) \right]. \quad (28)$$

The most significant deduction which can be made from equation (27) is that as  $z$  approaches  $-1$  (i.e.,  $a \rightarrow \infty$ ), the universe will be in TE if  $q < -1$ , provided  $\frac{dq}{dz}$  is finite. In our model, it can be readily seen that as  $z \rightarrow -1$ ,  $\frac{dq}{dz}$  diverges for  $\alpha > -1$ . Therefore, it is quite difficult to determine (analytically) the sign of  $\ddot{S}$  for our choices of  $\alpha$  as  $z \rightarrow -1$ . To remedy the situation, we have plotted  $\ddot{S}$  against the redshift  $z$  for the three chosen values of  $\alpha$  using Maple plotting software and presented them in figure 6. In doing so, we have used the best fit values of  $q_0$  and  $q_1$  obtained with each dataset as listed in tables I, II, and III. From the figure, it is clear that except for a slight discrepancy ( $\ddot{S} > 0$  in some future redshift interval) for  $\alpha = -0.5$  with the SNIa dataset,  $\ddot{S} < 0$  at all other instances during the final phases of evolution of the universe which is necessary for the TE to be satisfied. Hence, our proposed parametrization is well consistent with the GSL and TE and it provides a strong thermodynamic motivation for our study.



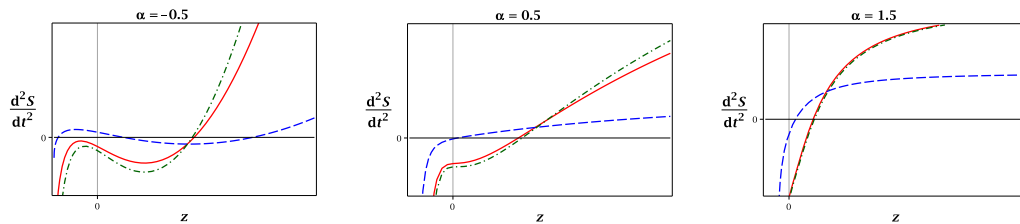


FIG. 6: The evolution of  $\ddot{S}$  is shown for the CC+ $H_0$  (red solid curves), SNIa (blue dashed curves) and SNIa+CC+ $H_0$  (green dashdot curves) datasets by considering different values of  $\alpha$ , as indicated in each panel.

## VI. CONCLUSIONS

In this paper, a parametric reconstruction of the deceleration parameter has been presented. The functional form of  $q$  is chosen in such a way that it reproduces three well-known  $q$ -parametrized models for  $\alpha = \pm 1$  and  $\alpha \rightarrow 0$ . The advantage of this type of parametrization is that it incorporates a wide class of viable models of cosmic evolution based on the choice of the parameter  $\alpha$ . We have also constrained the model parameters by  $\chi^2$  minimization technique using the CC+ $H_0$ , SNIa, and SNIa+CC+ $H_0$  datasets. We have shown that the constraints obtained on the parameter values by the joint (SNIa+CC+ $H_0$ ) analysis are very tight as compared to the constraints obtained from the SNIa dataset and the CC+ $H_0$  dataset independently. The corresponding results are presented in tables I, II, and III, while figure 1 shows the  $1\sigma$  and  $2\sigma$  confidence contours for our choices of the parameter  $\alpha$ . We have found that  $q(z)$  undergoes a smooth transition from a decelerated to an accelerated phase of expansion in the recent past. This result is essential to explain both the observed growth of structures at the early epoch and the current cosmic acceleration measurements. Also, the signature flip in  $q$  (from  $q > 0$  to  $q < 0$ ) occurs at the redshift  $z_t = 0.69^{+0.09}_{-0.06}$ ,  $0.65^{+0.10}_{-0.07}$ , and  $0.61^{+0.12}_{-0.08}$  within  $1\sigma$  errors for  $\alpha = -0.5$ ,  $0.5$ , and  $1.5$  respectively which are found to be well consistent with previous results [28, 32, 49–51], including the  $\Lambda$ CDM prediction ( $z_t \approx 0.7$ ). We therefore conclude that the present parameterized model provides the values for  $z_t$ ,  $q_0$  and  $w_{de}(z = 0)$ , which are in good agreement with recent observations for a wide range in the values of  $\alpha$ . Moreover, we have investigated whether our choice of parametrization is viable on thermodynamic grounds or not. To be specific, we have determined whether the GSL and the TE are satisfied in the course of evolution of the universe. We have found that our proposed model is well consistent with the GSL and TE, which provides a strong motivation for further studies of the model.

## VII. ACKNOWLEDGMENTS

The authors are thankful to Sudipta Das for a critical reading of the manuscript and providing useful comments and suggestions. SS was supported by SERB, Govt. of India under National Post-doctoral Fellowship Scheme [File No. PDF/2015/000906].

- 
- [1] Perlmutter S. et al., *Astrophys. J.*, **517**, 565 (1999).
  - [2] Riess A. G. et al., *Astron. J.*, **116**, 1009 (1998).
  - [3] Ade P. A. R. et al. [Planck Collaboration], *Phys. Rev. Lett.* **112**, 241101 (2014).
  - [4] Ade P. A. R. et al. [Planck Collaboration], *Phys. Rev. Lett.* **114**, 101301 (2015).
  - [5] Ade P. A. R. et al. [Planck Collaboration], *Phys. Rev. Lett.* **116**, 031302 (2016).
  - [6] Ade P. A. R. et al. [Planck Collaboration], *A&A*, **594**, A13 (2016).
  - [7] Ade P. A. R. et al. [Planck Collaboration], *A&A*, **594**, A20 (2016).
  - [8] Eisenstein D. J., *Astrophys. J.*, **633**, 560 (2005).
  - [9] Hinshaw G. et al., *Astrophys. J. Suppl.*, **208**, 19 (2013).
  - [10] Komatsu E. et al., *Astrophys. J. Suppl.*, **192**, 18 (2011).
  - [11] Seljak U. et al., *Phys. Rev. D.*, **71**, 103515 (2005).
  - [12] Tegmark M. et al., *Phys. Rev. D.*, **69**, 103501 (2004).
  - [13] Ade P. A. R. et al. [Planck Collaboration], *A & A*, **571**, A16 (2014).
  - [14] Ade P. A. R. et al. [Planck Collaboration], *A & A*, **571**, A24 (2014).
  - [15] Ade P. A. R. et al. [Planck Collaboration], *A & A*, **571**, A22 (2014).

- [16] Copeland E. J., Sami M., Tsujikawa S. Int. J. Mod. Phys. D, **15**, 1753 (2006).
- [17] Martin J., Mod. Phys. Lett. A, **23**, 1252 (2008).
- [18] Sahni V., Starobinsky A. A., Int. J. Mod. Phys. D, **9**, 373 (2000).
- [19] Sahni V., Lect. Notes Phys., **653**, 141 (2004).
- [20] Peebles P. J. E., Ratra B., Rev. Mod. Phys., **75**, 559 (2003).
- [21] Steinhardt P. J., et al., Phys. Rev. Lett., **59**, 123504 (1999).
- [22] Weinberg S., Rev. Mod. Phys., **61**, 1 (1989).
- [23] Turner M. S., Riess A. G., Astrophys. J., **569**, 18 (2002).
- [24] Aksaru O. et al., EPJ Plus, **129**, 22 (2014).
- [25] Cunha J. V., Lima J. A. S., MNRAS, **390**, 210 (2008).
- [26] Cunha J. V., Phys. Rev. D, **79**, 047301 (2009).
- [27] del Campo S. et al., Phys. Rev. D, **86**, 083509 (2012).
- [28] Nair R. et al., JCAP, **01**, 018 (2012).
- [29] Santos B., Carvalho J. C., Alcaniz J. S., Astropart. Phys., **35**, 17 (2011).
- [30] Gong Y., Wang A., Phys. Rev. D., **73**, 083506 (2006).
- [31] Gong Y., Wang A., Phys. Rev. D., **76**, 043520 (2007).
- [32] Mamon A. A., Das S., Int. J. Mod. Phys. D., **25**, 1650032 (2016).
- [33] Mamon A. A., Das S., arXiv: 1610.07337 [gr-qc] (2016).
- [34] Riess A. G., et al., Astrophys. J., **607**, 665 (2004).
- [35] Xu L., Liu H., Mod. Phys. Lett. A, **23**, 1939 (2008).
- [36] Xu L., Lu J., Mod. Phys. Lett. A, **24**, 369 (2009).
- [37] Bekenstein J. D. , Phys. Rev. D **7**, 2333 (1973).
- [38] Gibbons G., Hawking S. W., Phys. Rev. D **15**, 2738 (1977).
- [39] Jacobson T., Phys. Rev. Lett. **75**, 1260 (1995).
- [40] Padmanabhan T., Phys. Rep. **406**, 49 (2005).
- [41] Jimenez R., Loeb A., Astrophys. J., **573**, 37 (2002).
- [42] Moresco M. et al., JCAP, **05**, 014 (2016).
- [43] Moresco M., MNRAS, **450**, L16 (2015).
- [44] Simon J., Verde L., Jimenez R., Phys. Rev. D., **71**, 123001 (2005).
- [45] Stern D. et al., JCAP, **02**, 008 (2010).
- [46] Zhang C. et al., Res. Astron. Astrophys., **14**, 1221 (2014).
- [47] Betoule M. et al., A& A, **568**, A22 (2014).
- [48] Farooq O., Mania D., Ratra B., Astrophys. J., **764**, 138 (2013).
- [49] Farooq O., Ratra B., Astrophys. J., **766**, L7 (2013).
- [50] Magana J. et al., JCAP, **10**, 017 (2014).
- [51] Mamon A. A., Bamba K., Das S., Eur. Phys. J. C, **77**, 29 (2017).
- [52] Callen H. B., *Thermodynamics* (Wiley, NY) (1960).
- [53] Brustein R., Phys. Rev. Lett. **84**, 2072 (2000).
- [54] Wang B., Gong Y., Abdalla E., Phys. Rev. D., **74**, 083520 (2006).
- [55] Saha S., Chakraborty S., Phys. Lett. B., **717**, 319 (2012).
- [56] Saha S., Chakraborty S., Phys. Rev. D., **89**, 043512 (2014).